Second Data Release from the European Pulsar Timing Array: Challenging the Ultralight Dark Matter Paradigm

Clemente Smarra et al. (European Pulsar Timing Array)

Phys. Rev. Lett. **131**, 171001 — Published 25 October 2023

DOI: 10.1103/PhysRevLett.131.171001

The second data release from the European Pulsar Timing Array VI. Challenging the fuzzy dark matter paradigm

Clemente Smarra,[1,2,*] Boris Goncharov,[3,4] Enrico Barausse,[1,2] J. Antoniadis,[5,6] S. Babak,[7] A.-S. Bak Nielsen,[6,8] C. G. Bassa,[9] A. Berthereau,[10,11] M. Bonetti,[12,13,14] E. Bortolas,[12,13,14] P. R. Brook,[15] M. Burgay,[16] R. N. Caballero,[17] A. Chalumeau,[12] D. J. Champion,[6] S. Chanlaridis,[5] S. Chen,[18] I. Cognard,[10,11] G. Desvignes,[6] M. Falxa,[10,7] R. D. Ferdman,[19] A. Franchini,[12,13] J. R. Gair,[20] E. Graikou,[6] J.-M. Grießmeier,[10,11] L. Guillemot,[10,11] Y. J. Guo,[6] H. Hu,[6] F. Iraci,[16,21] D. Izquierdo-Villalba,[12,13] J. Jang,[6] J. Jawor,[6] G. H. Janssen,[9,22] A. Jessner,[6] R. Karuppusamy,[6] E. F. Keane,[23] M. J. Keith,[24] M. Kramer,[6,24] M. A. Krishnakumar,[6,8] K. Lackeos,[6] K. J. Lee,[5,6,11] K. Liu,[6] Y. Liu,[8,25] A. G. Lyne,[24] J. W. McKee,[26,27] R. A. Main,[6] M. B. Mickaliger,[24] I. C. Niţu,[24] A. Parthasarathy,[6] B. B. P. Perera,[28] D. Perrodin,[16] A. Petiteau,[29,7] N. K. Porayko,[6,12] A. Possenti,[16] H. Quelquejay Leclere,[7] A. Samajdar,[30] S. A. Sanidas,[24] A. Sesana,[12,13,14] G. Shaifullah,[12,13,16] L. Speri,[20] R. Spiewak,[24] B. W. Stappers,[24] S. C. Susarla,[31] G. Theureau,[10,11,32] C. Tiburzi,[16] E. van der Wateren,[22,9] A. Vecchio,[15] V. Venkatraman Krishnan,[6] J. Wang,[8,33,34] L. Wang,[24] and Z. Wu[25]

(The European Pulsar Timing Array)

[1] *SISSA — International School for Advanced Studies, Via Bonomea 265, 34136, Trieste, Italy and INFN, Sezione di Trieste*

[2] *IFPU — Institute for Fundamental Physics of the Universe, Via Beirut 2, 34014 Trieste, Italy*

[3] *Gran Sasso Science Institute (GSSI), I-67100 L'Aquila, Italy*

[4] *INFN, Laboratori Nazionali del Gran Sasso, I-67100 Assergi, Italy*

[5] *Institute of Astrophysics, FORTH, N. Plastira 100, 70013, Heraklion, Greece*

[6] *Max-Planck-Institut für Radioastronomie, Auf dem Hügel 69, 53121 Bonn, Germany*

[7] *Université Paris Cité CNRS, Astroparticule et Cosmologie, 75013 Paris, France*

[8] *Fakultät für Physik, Universität Bielefeld, Postfach 100131, 33501 Bielefeld, Germany*

[9] *ASTRON, Netherlands Institute for Radio Astronomy, Oude Hoogeveensedijk 4, 7991 PD, Dwingeloo, The Netherlands*

[10] *Laboratoire de Physique et Chimie de l'Environnement et de l'Espace, Université d'Orléans / CNRS, 45071 Orléans Cedex 02, France*

[11] *Observatoire Radioastronomique de Nançay, Observatoire de Paris, Université PSL, Université d'Orléans, CNRS, 18330 Nançay, France*

[12] *Dipartimento di Fisica "G. Occhialini", Universitá degli Studi di Milano-Bicocca, Piazza della Scienza 3, I-20126 Milano, Italy*

[13] *INFN, Sezione di Milano-Bicocca, Piazza della Scienza 3, I-20126 Milano, Italy*

[14] *INAF - Osservatorio Astronomico di Brera, via Brera 20, I-20121 Milano, Italy*

[15] *Institute for Gravitational Wave Astronomy and School of Physics and Astronomy, University of Birmingham, Edgbaston, Birmingham B15 2TT, UK*

[16] *INAF - Osservatorio Astronomico di Cagliari, via della Scienza 5, 09047 Selargius (CA), Italy*

[17] *Hellenic Open University, School of Science and Technology, 26335 Patras, Greece*

[18] *Kavli Institute for Astronomy and Astrophysics, Peking University, Beijing 100871, P. R. China*

[19] *School of Physics, Faculty of Science, University of East Anglia, Norwich NR4 7TJ, UK*

[20] *Max Planck Institute for Gravitational Physics (Albert Einstein Institute), Am Muühlenberg 1, 14476 Potsdam, Germany*

[21] *Universitá di Cagliari, Dipartimento di Fisica, S.P. Monserrato-Sestu Km 0,700 - 09042 Monserrato (CA), Italy*

[22] *Department of Astrophysics/IMAPP, Radboud University Nijmegen, P.O. Box 9010, 6500 GL Nijmegen, The Netherlands*

[23] *School of Physics, Trinity College Dublin, College Green, Dublin 2, D02 PN40, Ireland*

[24] *Jodrell Bank Centre for Astrophysics, Department of Physics and Astronomy, University of Manchester, Manchester M13 9PL, UK*

[25] *National Astronomical Observatories, Chinese Academy of Sciences, Beijing 100101, P. R. China*

[26] *E.A. Milne Centre for Astrophysics, University of Hull, Cottingham Road, Kingston-upon-Hull, HU6 7RX, UK*

[27] *Centre of Excellence for Data Science, Artificial Intelligence and Modelling (DAIM), University of Hull, Cottingham Road, Kingston-upon-Hull, HU6 7RX, UK*

[28] *Arecibo Observatory, HC3 Box 53995, Arecibo, PR 00612, USA*

[29] *IRFU, CEA, Université Paris-Saclay, F-91191 Gif-sur-Yvette, France*

[30] *Institut für Physik und Astronomie, Universität Potsdam, Haus 28, Karl-Liebknecht-Str. 24/25, 14476, Potsdam, Germany*

[31] *Ollscoil na Gaillimhe — University of Galway, University Road, Galway, H91 TK33, Ireland*

[32] *Laboratoire Univers et Théories LUTh, Observatoire de Paris, Université PSL, CNRS, Université de Paris, 92190 Meudon, France*
[33] *Ruhr University Bochum, Faculty of Physics and Astronomy, Astronomical Institute (AIRUB), 44780 Bochum, Germany*
[34] *Advanced Institute of Natural Sciences, Beijing Normal University, Zhuhai 519087, China*
(Dated: September 15, 2023)

Pulsar Timing Array experiments probe the presence of possible scalar/pseudoscalar ultralight dark matter particles through decade-long timing of an ensemble of galactic millisecond radio pulsars. With the second data release of the European Pulsar Timing Array, we focus on the most robust scenario, in which dark matter interacts only gravitationally with ordinary baryonic matter. Our results show that ultralight particles with masses $10^{-24.0}$ eV $\lesssim m \lesssim 10^{-23.3}$ eV cannot constitute 100% of the measured local dark matter density, but can have at most local density $\rho \lesssim 0.3$ GeV/cm^3.

Introduction.—The nature of Dark Matter (DM) is arguably one of the most fascinating and mysterious questions that we are struggling to answer. Galaxy rotation curves [1, 2], the peculiar motion of clusters [3, 4], the Bullet Cluster system [5], measurements of cosmological abundances from Cosmic Microwave Background (CMB) and Baryonic Acoustic Oscillation (BAO) observations [6, 7] all point to the existence of a hitherto-unseen type of matter, constituting roughly 26% of the current energy density of the Universe and interacting mostly gravitationally with the Standard Model of particle physics. The standard Cold Dark Matter (CDM) paradigm describes successfully many aspects of the large-scale structure of the Universe, but struggles to predict what we observe at scales smaller than the ∼kpc. For instance, observations favor a constant density profile in the inner part of galaxies, while CDM predicts a steep power-law-like behavior (*cusp-core problem*) [8–10]. Furthermore, well-known issues are associated with the discrepancy between the observed and expected number of Milky Way (MW) satellites (*missing satellite problem*) [11, 12] and with ΛCDM simulations showing that the most massive subhaloes of the MW would be too dense to host any of its bright satellites (*too-big-to-fail problem*) [13]. Moreover, recent anomalies in gravitationally lensed images [14] seem to disfavor the long-standing Weakly-Interacting-Massive-Particles (WIMPs) hypothesis for CDM. While some of these issues might be alleviated by invoking baryonic feedback mechanisms [15], e.g. Active Galactic Nuclei (AGN) [16] and/or supernova feedback [17–22], it is still unclear how the flat density profile of dwarf galaxies (e.g. Fornax [23]), with almost no baryonic activity in the center, can be explained without invoking a novel mechanism. An intriguing alternative is to consider the possibility that DM is fuzzy, *i.e.* an ultra-light scalar field ($m_\phi \sim 10^{-22}$ eV) or axion-like particle, whose wavelike nature suppresses structure formation on scales smaller than the de Broglie wavelength, while maintaining all the achievements of the CDM paradigm on large scales. Moreover, the existence of ultralight scalars can also be motivated on a more theoretical ground: in particular, axion-like particles generically arise in string theory compactifications as Kaluza–Klein zero modes of antisymmetric tensor fields [24–26].

A wealth of studies have been carried out to probe the existence of ultra-light dark matter (ULDM), ranging from CMB observables to Lyman-α and stellar kinematics. Specifically, the integrated Sachs-Wolfe effect on CMB anisotropies rules out masses $m_\phi \lesssim 10^{-24}$ eV [27], while Lyman-α gives a lower bound $m_\phi \gtrsim 10^{-21}$ eV for ultra-light candidates constituting more than $\sim 30\%$ of DM[1] [28–32]. Stellar orbit kinematics in ultra-faint dwarf (UFD) galaxies might even be able to bound the scalar field mass to be $m_\phi \gtrsim 10^{-19}$ eV, although this is still under debate [33, 34]. However, the sensitivity of non-CMB constraints to uncertainties in the modeling of small scale structure properties [35, 36] makes it compelling to rely on complementary and independent probes. It was shown by Khmelnitsky and Rubakov [37] that the presence of ULDM induces an oscillating gravitational potential that affects the light travel time of radio pulses emitted by pulsars. Therefore, Pulsar Timing Arrays (PTAs) stand out as promising experiments to test the presence of ULDM particles in the MW. Previous PTA searches placed 95% upper limits on the local energy density of ULDM at 3×10^{-24} eV to $\lesssim 1$ GeV/cm^3 [38–40].

In this work, which is complementary to the European Pulsar Timing Array (EPTA) interpretation effort [41], we focus on a specific range of ULDM masses and constrain the local ULDM density to values *below* the observed local DM density. We do so by analyzing the effect of ULDM on the times of arrival (TOAs) of pulsar radio beams. Therefore, if ULDM particles exist in the mass range that we consider, they cannot constitute all of the observed DM.

Models.—As we only have gravitational evidence of DM, we focus on an ultra-light scalar field with negligible self-interactions and no couplings with the Standard Model. The action for this field can be written as

$$S = \int d^4x\sqrt{-g}\left[\frac{1}{2}g^{\mu\nu}\partial_\mu\phi\partial_\nu\phi - \frac{1}{2}m_\phi^2\phi^2\right]. \quad (1)$$

* csmarra@sissa.it

[1] Notice, however, that the value of the fraction of ULDM compatible with Lyman-α is extrapolated for masses $m_\phi \lesssim 10^{-22}$ eV.

Due to its high occupation number and non-relativistic nature, the ULDM scalar field can be thought as a classical wave [37]:

$$\phi(\vec{x},t) = \frac{\sqrt{2\rho_\phi}}{m_\phi}\hat{\phi}(\vec{x})\cos\left(m_\phi t + \gamma(\vec{x})\right), \tag{2}$$

where m_ϕ is the mass of the scalar field, $\gamma(\vec{x})$ is a space-dependent phase and $\hat{\phi}(\vec{x})$ accounts for the pattern of interference in the proximity of $\vec{x}$ caused by the wave-like nature of ULDM. The scalar field density ρ_ϕ is conveniently normalized to the local DM density $\rho_{\rm DM}$, which can be determined e.g. by fitting the MW rotation curve or, in a more refined way, by studying the vertical oscillations of disc stars [42–45]. In the following, we assume a fiducial value $\rho_{\rm DM} \approx 0.4$ GeV/cm^3. The oscillating nature of ULDM induces an oscillating gravitational potential leading to a periodic displacement $\delta t_{\rm DM}$ in the TOAs of radio pulses emitted by pulsars, which can be written as [37, 39]:

$$\delta t_{\rm DM} = \frac{\Psi_{\rm c}(\vec{x})}{2m_\phi}[\hat{\phi}^2_{\rm E}\sin\left(2m_\phi + \gamma_{\rm E}\right) - \hat{\phi}^2_{\rm P}\sin\left(2m_\phi + \gamma_{\rm P}\right)], \tag{3}$$

where

$$\frac{\Psi_{\rm c}(\vec{x})}{10^{-18}} \approx 6.52\left(\frac{10^{-22}\ {\rm eV}}{m_\phi}\right)^2\left(\frac{\rho_\phi}{0.4\ {\rm GeV/cm^3}}\right), \tag{4}$$

and $\gamma_{\rm P} \equiv 2\gamma(\vec{x_{\rm p}}) - 2m_\phi d_p/c$ ($\gamma_{\rm E} \equiv 2\gamma(\vec{x_{\rm e}})$) are related to the phases of Eq. (2) evaluated at the pulsar (Earth) location, with d_p standing for the pulsar-Earth distance. The amplitude in Eq. (4) is computed assuming a constant DM density background and possible deviations caused by the wave-like nature of the ultralight scalar field are parametrized in terms of the pulsar (Earth) dependent phase factors $\hat{\phi}^2(\vec{x_{\rm p}}) \equiv \hat{\phi}^2_{\rm P}$ ($\hat{\phi}^2(\vec{x_{\rm e}}) \equiv \hat{\phi}^2_{\rm E}$). The approximation of constant DM density across pulsars is sufficient, as their distances from Earth are all ∼kpc and subject to large measurement uncertainties [39]. Notice that accurate measurements of pulsar-Earth distances might help to reduce the number of free parameters in the limit in which $\gamma(\vec{x_{\rm p}}) = \gamma(\vec{x_{\rm e}})$. Moreover, precise determination of pulsar positions could provide us with more information about the dark matter density in its surroundings. On scales smaller than the de Broglie wavelength, the ULDM scalar field oscillates coherently, with the same amplitude $\hat{\phi}$ (see Eq. (2)). Since the typical ULDM velocity is expected to be $v_\phi \sim 10^{-3}$, the coherence length is approximately

$$l_c \approx \frac{2\pi}{m_\phi v_\phi} \approx 0.4\ {\rm kpc}\left(\frac{10^{-22}\ {\rm eV}}{m_\phi}\right). \tag{5}$$

Therefore, $\hat{\phi}^2_{\rm E}$ and $\hat{\phi}^2_{\rm P}$ are:

- *uncorrelated* if the coherence length of ULDM is less than the average inter-pulsar and pulsar-Earth separation. In this case, $\hat{\phi}^2_{\rm E}$ and $\hat{\phi}^2_{\rm P}$ will thus be separate parameters;
- *correlated* if the coherence length of ULDM is larger than the inter-pulsar and pulsar-Earth separations and encloses the typical Galacto-centric region tested by the most precise MW rotation curves measurements (roughly the inner ∼ 20 kpc [46]). In this case, $\hat{\phi}^2_{\rm E} = \hat{\phi}^2_{\rm P}$ for all the pulsars. Moreover, rotation curves also sample from the same coherence patch, and thus measure the local abundance $\rho_{\rm DM}$ of DM. Therefore, the stochastic parameter $\hat{\phi}^2$ can be safely absorbed in a redefinition of $\Psi_{\rm c}$.
- *pulsar-correlated* if the coherence length of ULDM is larger than the inter-pulsar and pulsar-Earth separations, but smaller than the typical Galacto-centric radius sampled by rotation curves. In this case, $\hat{\phi}^2_{\rm E} = \hat{\phi}^2_{\rm P}$ for all the pulsars. However, DM density estimates from rotation curves average over different patches. We therefore keep $\hat{\phi}^2$ as a free parameter and consistently marginalize over it. In this way, the limits on $\rho_{\rm DM}$ obtained from pulsars will constrain the same quantity measured by rotation curves.

We perform the analysis in the three limits above, noting that the fully correlated limit has not been considered in the previous studies [47, 48]. From Eq. (5), recalling that the pulsar-Earth distance is $\mathcal{O}$(kpc) for the observed systems, it follows that the *correlated* regime is an excellent approximation for masses lower than $m_\phi \sim 2\times10^{-24}$ eV; the *pulsar-correlated* regime holds for $2\times10^{-24}\,{\rm eV} \lesssim m_\phi \lesssim 5\times10^{-23}\,{\rm eV}$ and the *uncorrelated* regime is valid for $m_\phi \gtrsim 5\times10^{-23}$ eV.

Dataset and methodology.—The EPTA monitors 42 millisecond radio pulsars with five telescopes located in France, Germany, Italy, the Netherlands, and the United Kingdom. The second data release (DR2) of the EPTA contains 24.7 years of observations of pulse arrival times of 25 pulsars, surveyed with an approximate cadence of once every 3 weeks [49], which translates into a Nyquist frequency of approximately 3×10^{-7} Hz. TOAs are measured at the position of the Solar System Barycenter, and are primarily described by pulsar-specific deterministic timing models accounting for the position of each pulsar in the sky, spin down, proper motion, the presence of a binary companion, etc. The timing models are provided with the data set. Deviations between the TOAs predicted by these models and the measured TOAs are referred to as the timing residuals, δt. The residuals contain contributions from various sources of noise, from variations in the dispersion measure to irregularities in pulsar rotation, but they may also contain signals of astrophysical interest. The sources of noise are identified as part of the noise analysis of the EPTA DR2 [50]. The DR2 data set also hints at growing evidence for the stochastic gravitational-wave background, which manifests itself as a temporally-correlated stochastic process with a hallmark inter-pulsar correlation signature of General Relativity [51]. Our work is complementary to the

EPTA-wide interpretation effort of the spatial and temporal correlations in DR2 [41].

We use Bayesian inference techniques to search for the ULDM signal while simultaneously fitting timing model parameters and all known sources of noise to the data, to correctly marginalize over the associated uncertainties. The likelihood of the timing residuals, $\mathcal{L}(\delta t|\theta)$, given the parameters of the models, θ, is [52–56]

$$\ln \mathcal{L}(\delta t|\theta) \propto -\frac{1}{2}(\delta t-\mu)^{\mathrm{T}} C^{-1}(\delta t-\mu). \tag{6}$$

This is a time-domain Gaussian likelihood, multivariate with respect to a number of observations, *i.e.*, δt has dimension equal to the number of observations. The contribution of ULDM from Eq. (3) is added to μ, which also contains contributions from the timing model [49] and noise processes, according to the noise analysis of Ref. [50]. The diagonal part of the covariance matrix C contains TOA measurement uncertainties that include temporally-uncorrelated "white" noise. Contributions from temporally correlated "red" noise may be added as off-diagonal elements in C. However, for computational efficiency, red noise contributions are modeled in μ [53, 54]. The priors $\pi(\theta)$ are set based on Table I, see Ref. [47] for further details. To obtain a sufficient amount of posterior samples across the mass-frequency parameter space, the search is effectively performed across equally-spaced segments of $\pi(m_\phi)$, which we refer to as bins. The measurements of parameters are obtained as posterior distributions, $\mathcal{P}(\theta|d) \propto \mathcal{L}(\delta t|\theta)\pi(\theta)$. The posteriors are evaluated using the Parallel-Tempering-Markov-Chain Monte-Carlo sampler [57] implemented in ENTERPRISE [55] and ENTERPRISE_EXTENSIONS [56] . The conclusion about the presence or absence of the ULDM signal in the data is based on the Bayesian odds ratio. In our case, that is equal to the Bayes factor, because we assume the prior odds of both scenarios to be equal. We evaluate Bayes factors, $\mathcal{B}$, using the Savage-Dickey density ratio [58]. In particular, finding $\ln \mathcal{B} \gtrsim 5$ would indicate robust evidence for the ULDM signal.

There is strong evidence for a temporally-correlated red signal in EPTA DR2, characterized by the same Fourier spectrum of δt in all pulsars [51]. This signal may contain contributions from the stochastic gravitational-wave background [59]. Because in the 24.7-yr data set this signal does not show significant evidence for inter-pulsar correlations (unlike in the 10.3-yr data set [41, 49–51]), we model it as a spatially uncorrelated red noise process. Individual Fourier components of this broad-band signal may contaminate frequencies at which the presence of ULDM is evaluated. Thus, this common red noise signal is included in the null hypothesis, $\varnothing$, along with the pulsar-intrinsic noise. The signal hypothesis is based on adding ULDM to the null hypothesis.

Results.—We carry out the search for ULDM in the correlated, pulsar-correlated and uncorrelated limit for $\hat{\phi}^2_{\mathrm{E}}$ and $\hat{\phi}^2_{\mathrm{P}}$ with the parameters in Table I. The factors $\hat{\phi}^2_{\mathrm{E}}$ and $\hat{\phi}^2_{\mathrm{P}}$ are drawn from an exponential prior, to correctly model the stochastic nature of the ULDM field [60, 61]. We find no evidence for a signal in the mass range $m_\phi \sim [10^{-24}\ \mathrm{eV}, 10^{-22}\ \mathrm{eV}]$. The largest $\ln \mathcal{B}$ we find across frequency-mass bins is < 1, i.e. the null hypothesis is favored. Therefore, we calculate the 95% upper limits on the signal amplitude Ψ_{c} and, through Eq. (4), on the scalar field density ρ_ϕ. The results are shown in Fig. 1.

A highlight of our study is that not only does EPTA DR2 yield more stringent constraints than previous results [38, 39], but it also rules out that particles with masses $m_\phi \sim [10^{-24}\ \mathrm{eV}, 10^{-23.3}\ \mathrm{eV}]$ can be 100% of the observed local DM density. In particular, the scalar field density is $\rho_\phi \lesssim 0.15\ \mathrm{GeV/cm^3}$ in the mass range $m_\phi \sim [10^{-24}\ \mathrm{eV}, 10^{-23.7}\ \mathrm{eV}]$, while it is constrained to $\rho_\phi \lesssim 0.30\ \mathrm{GeV/cm^3}$ between $m_\phi \sim [10^{-23.7}\ \mathrm{eV}, 10^{-23.4}\ \mathrm{eV}]$. Furthermore, the correlated limit in Fig. 1 confirms Lyman-α bounds, which exclude ULDM in this mass range unless it constitutes less than 30% of DM [30]. It is worth noticing that the low-frequency end of Fig. 1 extends below the näive expectation $f = 1.3$ nHz corresponding to the inverse of the observation time $T_{\mathrm{obs}} = 24.7$ yr. In fact, while an ULDM candidate in this mass region does not complete an oscillation cycle during the observation timescale, the signal can still be approximated by a polynomial expansion in $(m_\phi t)$ [47]. The sensitivity in this region is limited by the simultaneous fitting to pulsar spin frequency derivatives [62, 63]. PTAs are only sensitive to the $(m_\phi t)^3$ term, as the first terms in the expansion are degenerate with the timing model [64]. However, since the expected amplitude Ψ_{c} of an ULDM candidate increases as its mass decreases, we can still obtain competitive constraints at low frequency. While, in principle, our analysis could be pushed to even lower masses [65], we choose to focus on the region $m_\phi \gtrsim 10^{-24}$ eV to comply with the aforementioned CMB bounds. We find that the significant improvement in sensitivity to ULDM at low frequencies arises thanks to the larger data span of EPTA DR2, in accordance with the theoretical sensitivity scaling proposed in Eq. (13) of Ref. [65]. In particular, because of the longer data span, we expect EPTA DR2 limits to be better than NANOGrav [66] ones by a factor of roughly ~ 3.6, which is in agreement with what observed. At high frequencies, we find that the advantage of the long timing baseline compared to NANOGrav diminishes, also in accordance with the scaling, as pulsar white noise levels become more important. We also performed an identical analysis of the 10-year subset of EPTA DR2 [49, 51], as well as of the MeerTime data [67], which yield less stringent upper limits in agreement with the scaling. For comparison, the bounds in both the correlated and uncorrelated limit for the 10-year subset of the EPTA, shown in Fig. 22 in Ref. [41], appear at the level of the pulsar-correlated limit in Fig. 1 of this manuscript.

In the following, we clarify some specific aspects of our results. First, we notice that a similar analysis has been done by the North American Nanohertz Observatory for Gravitational Waves (NANOGrav) collaboration [66].

TABLE I: Parameters employed for the search along with their respective priors. In the correlated limit, the parameters $\hat{\phi}^2_{\rm E}, \hat{\phi}^2_{\rm P}$ are accounted for by a redefinition of Ψ_c, while in the pulsar-correlated regime $\hat{\phi}^2_{\rm E} = \hat{\phi}^2_{\rm P} = \hat{\phi}^2$ is a free parameter.

Parameter	**Description**	**Prior**	**Occurrence**
White Noise $(\sigma = E_{\rm f}^2\sigma^2_{\rm TOA} + E^2_{\rm q})$			
$E_{\rm f}$	EFAC per backend/receiver system	Uniform $[0, 10]$	1 per pulsar
$E_{\rm q}$	EQUAD per backend/receiver system	$\rm Log_{10}$-Uniform $[-10, -5]$	1 per pulsar
Red Noise			
$A_{\rm red}$	Red noise power-law amplitude	$\rm Log_{10}$-Uniform $[-20, -6]$	1 per pulsar
$\gamma_{\rm red}$	Red noise power-law spectral index	Uniform $[0, 10]$	1 per pulsar
ULDM			
$\Psi_{\rm c}$	ULDM signal amplitude	$\rm Log_{10}$-Uniform $[-20, -12]$	1 per PTA
m_ϕ [eV]	ULDM mass	$\rm Log_{10}$-Uniform $[-24, -22]$	1 per PTA
$\hat{\phi}^2_{\rm E}$	Earth factor	e^{-x}	1 per PTA
$\hat{\phi}^2_{\rm P}$	Pulsar factor	e^{-x}	1 per pulsar
$\gamma_{\rm E}$	Earth signal phase	Uniform $[0, 2\pi]$	1 per PTA
$\gamma_{\rm P}$	Pulsar signal phase	Uniform $[0, 2\pi]$	1 per pulsar
Common spatially Uncorrelated Red Noise (CURN)			
$A_{\rm GWB}$	Common process strain amplitude	$\rm Log_{10}$-Uniform $[-20, -6]$	1 per PTA

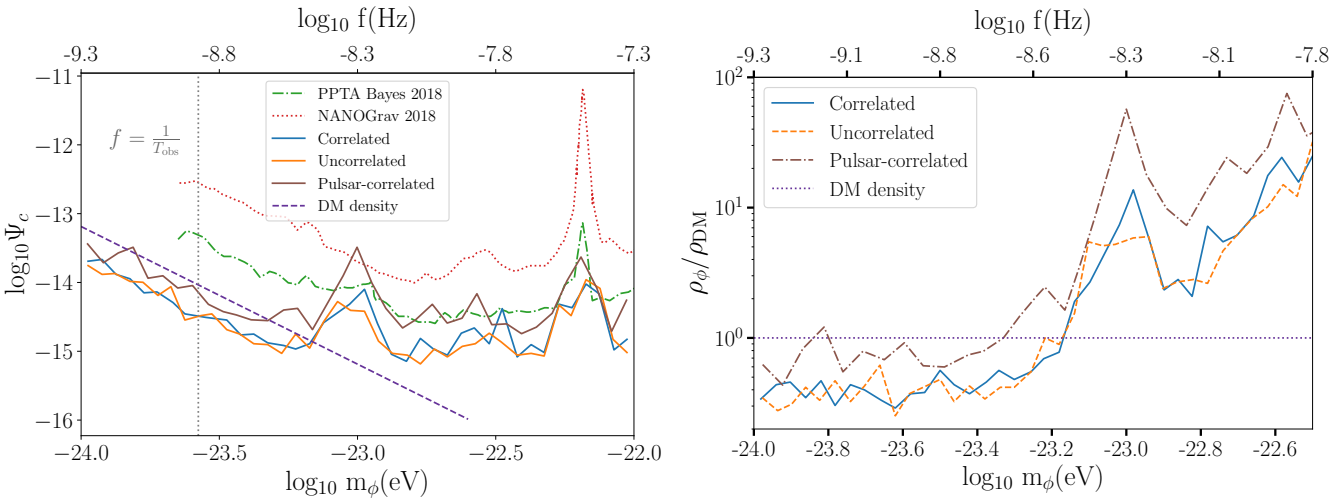

FIG. 1: Upper limits on ULDM, and namely on the dimensionless amplitude ($\Psi_{\rm c}$, *left panel*) and the ULDM fraction of the local DM density $\rho_{\rm DM} = 0.4{\rm GeV/cm}^3$ ($\rho_\phi/\rho_{\rm DM}$, *right panel*), at 95% credibility. The bottom horizontal axes show the ULDM particle mass, whereas the top horizontal axes show the equivalent oscillation frequency of the scalar field. The upper limits from previous searches [38, 39] are shown for comparison. As a reference, we highlight the frequency $T^{-1}_{\rm obs}$. In the right panel, we zoom in on the excluded ULDM masses. The horizontal dotted line represents the value of ρ_ϕ that would saturate the local DM density. Notice that based on our results ULDM particles with mass $-24.0 < \log_{10}\,(m_\phi/{\rm eV}) < -23.7$ can only make up at most $30 - 40$ % of the total DM energy density, while particles with mass $-23.7 < \log_{10}\,(m_\phi/{\rm eV}) < -23.3$ can contribute at most up to ~ 70 %.

There, the upper limits provided in the correlated and uncorrelated scenarios differ at low frequency. This can be understood by noticing that the correlated limit of NANOGrav corresponds to our pulsar-correlated limit. However, in the low mass limit of Fig. 1, the pulsars, the Earth and the stellar and gaseous tracers used for rotation curves estimates lie well within the area spanned by the coherence length; thus, one can only measure the combination $\Psi^0_c = \Psi_c\hat{\phi}^2$, which represents the realization of DM in our Galaxy. Therefore, we remove the

$\hat{\phi}_{\rm E}^2 = \hat{\phi}_{\rm P}^2 \equiv \hat{\phi}^2$ parameter in the correlated limit, as it can be accounted for by a redefinition of Ψ_c. Fitting for Ψ_c and $\hat{\phi}^2$ separately, instead, introduces an additional uncertainty, which leads our pulsar-correlated analysis to produce a similar mismatch as the one found in Ref. [66], as shown in Fig. 1. Second, Fig. 1 hints at a steep increase in the upper limits at $m_\phi \gtrsim 10^{-23.2}$ eV. In fact, we report the presence of excess signal power on top of the common red noise process, corresponding to a mass of $m_\phi \simeq 10^{-23}$ eV and an amplitude of $\Psi_{\rm c} \simeq 6 \times 10^{-14}$ or, equivalently, a density of $\rho_\phi = 40$ GeV/cm^3. At face value, this excess is not compatible with an ULDM candidate, as the corresponding density is outside the local DM measurement uncertainties [42–45]. Moreover, such a mass would be in tension with astrophysical bounds, as extensively discussed in the introduction [27–34]. Anyway, the Bayesian odds ratio suggests that it is still consistent with noise ($\ln \mathcal{B} \sim 0.1$). We find a similar excess in the analysis of 10-yr subset of the EPTA DR2 [41]. Moreover, the boson mass corresponding to the excess also matches the frequency of the continuous gravitational wave (CGW) candidate studied in [68]. This motivates further investigations as part of the International Pulsar Timing Array [69].

Conclusions.— ULDM is a theoretically motivated paradigm that may alleviate the *small-scale crisis* of structure formation. Here, we focused on the most robust scenario, in which ULDM features only gravitational interactions. These interactions produce a periodic oscillation in the TOAs of the radio beams emitted by pulsars, which can then be collected in PTA telescopes. PTAs stand out as excellent laboratories to test the effects of ULDM in the mass range $m_\phi \sim [10^{-24}\ {\rm eV}, 10^{-22}\ {\rm eV}]$. In this work, we showed that PTAs constrain the presence of ULDM *below* a few tenths of the observed DM abundance in the mass range $m_\phi \sim [10^{-24}\ {\rm eV}, 10^{-23.3}\ {\rm eV}]$. Therefore, in this range, ULDM cannot constitute 100% of the observed DM.

We wish to thank Diego Blas, Alessio Zicoschi and Paolo Salucci for useful discussions and insights. CS and EB acknowledge support from the European Union's H2020 ERC Consolidator Grant "GRavity from Astrophysical to Microscopic Scales" (Grant No. GRAMS-815673) and the EU Horizon 2020 Research and Innovation Programme under the Marie Sklodowska-Curie Grant Agreement No. 101007855. BG is supported by the Italian Ministry of Education, University and Research within the PRIN 2017 Research Program Framework, n. 2017SYRTCN. The European Pulsar Timing Array (EPTA) is a collaboration between European and partner institutes, namely ASTRON (NL), INAF/Osservatorio di Cagliari (IT), Max-Planck-Institut für Radioastronomie (GER), Nançay/Paris Observatory (FRA), the University of Manchester (UK), the University of Birmingham (UK), the University of East Anglia (UK), the University of Bielefeld (GER), the University of Paris (FRA), the University of Milan-Bicocca (IT), the Foundation for Research and Technology, Hellas (GR), and Peking University (CHN), with the aim to provide high-precision pulsar timing to work towards the direct detection of low-frequency gravitational waves. An Advanced Grant of the European Research Council allowed to implement the Large European Array for Pulsars (LEAP) under Grant Agreement Number 227947 (PI M. Kramer). The EPTA is part of the International Pulsar Timing Array (IPTA); we thank our IPTA colleagues for their support and help with this paper and the external Detection Committee members for their work on the Detection Checklist. The work presented here is a culmination of many years of data analysis as well as software and instrument development. In particular, we thank Drs. N. D'Amico, P. C. C. Freire, R. van Haasteren, C. Jordan, K. Lazaridis, P. Lazarus, L. Lentati, O. Löhmer and R. Smits for their past contributions. We also thank Dr. N. Wex for supporting the calculations of the galactic acceleration as well as the related discussions. The EPTA is also grateful to staff at its observatories and telescopes who have made the continued observations possible. Part of this work is based on observations with the 100-m telescope of the Max-Planck-Institut für Radioastronomie (MPIfR) at Effelsberg in Germany. Pulsar research at the Jodrell Bank Centre for Astrophysics and the observations using the Lovell Telescope are supported by a Consolidated Grant (ST/T000414/1) from the UK's Science and Technology Facilities Council (STFC). ICN is also supported by the STFC doctoral training grant ST/T506291/1. The Nançay radio Observatory is operated by the Paris Observatory, associated with the French Centre National de la Recherche Scientifique (CNRS), and partially supported by the Region Centre in France. We acknowledge financial support from "Programme National de Cosmologie and Galaxies" (PNCG), and "Programme National Hautes Energies" (PNHE) funded by CNRS/INSU-IN2P3-INP, CEA and CNES, France. We acknowledge financial support from Agence Nationale de la Recherche (ANR-18-CE31-0015), France. The Westerbork Synthesis Radio Telescope is operated by the Netherlands Institute for Radio Astronomy (ASTRON) with support from the Netherlands Foundation for Scientific Research (NWO). The Sardinia Radio Telescope (SRT) is funded by the Department of University and Research (MIUR), the Italian Space Agency (ASI), and the Autonomous Region of Sardinia (RAS) and is operated as a National Facility by the National Institute for Astrophysics (INAF). The work is supported by the National SKA programme of China (2020SKA0120100), Max-Planck Partner Group, NSFC 11690024, CAS Cultivation Project for FAST Scientific. This work is also supported as part of the "LEGACY" MPG-CAS collaboration on low-frequency gravitational wave astronomy. JA acknowledges support from the European Commission (Grant Agreement number: 101094354). JA and SCha were partially supported by the Stavros Niarchos Foundation (SNF) and the Hellenic Foundation for Research and Innovation (H.F.R.I.) under the 2nd Call of the "Sci-

ence and Society – Action Always strive for excellence – Theodoros Papazoglou" (Project Number: 01431). AC acknowledges support from the Paris Île-de-France Region. AC, AF, ASe, ASa, EB, DI, GMS, MBo acknowledge financial support provided under the European Union's H2020 ERC Consolidator Grant "Binary Massive Black Hole Astrophysics" (B Massive, Grant Agreement: 818691). GD, KLi, RK and MK acknowledge support from European Research Council (ERC) Synergy Grant "BlackHoleCam", Grant Agreement Number 610058. This work is supported by the ERC Advanced Grant "LEAP", Grant Agreement Number 227947 (PI M. Kramer). AV and PRB are supported by the UK's Science and Technology Facilities Council (STFC; grant ST/W000946/1). AV also acknowledges the support of the Royal Society and Wolfson Foundation. JPWV acknowledges support by the Deutsche Forschungsgemeinschaft (DFG) through thew Heisenberg programme (Project No. 433075039) and by the NSF through AccelNet award #2114721. NKP is funded by the Deutsche Forschungsgemeinschaft (DFG, German Research Foundation) – Projektnummer PO 2758/1–1, through the Walter–Benjamin programme. ASa thanks the Alexander von Humboldt foundation in Germany for a Humboldt fellowship for postdoctoral researchers. APo, DP and MBu acknowledge support from the research grant "iPeska" (P.I. Andrea Possenti) funded under the INAF national call Prin-SKA/CTA approved with the Presidential Decree 70/2016 (Italy). RNC acknowledges financial support from the Special Account for Research Funds of the Hellenic Open University (ELKE-HOU) under the research programme "GRAVPUL" (grant agreement 319/10-10-2022). EvdW, CGB and GHJ acknowledge support from the Dutch National Science Agenda, NWA Startimpuls – 400.17.608. LS acknowledges the use of the HPC system Cobra at the Max Planck Computing and Data Facility.

[1] Vera C. Rubin and Jr. Ford, W. Kent. Rotation of the Andromeda Nebula from a Spectroscopic Survey of Emission Regions. *ApJ*, 159:379, February 1970. doi: 10.1086/150317.

[2] V. C. Rubin, Jr. Ford, W. K., and N. Thonnard. Rotational properties of 21 SC galaxies with a large range of luminosities and radii, from NGC 4605 (R=4kpc) to UGC 2885 (R=122kpc). *ApJ*, 238:471–487, June 1980. doi:10.1086/158003.

[3] F. Zwicky. Die Rotverschiebung von extragalaktischen Nebeln. *Helvetica Physica Acta*, 6:110–127, January 1933.

[4] F. Zwicky. On the Masses of Nebulae and of Clusters of Nebulae. *ApJ*, 86:217, October 1937. doi:10.1086/143864.

[5] Douglas Clowe, Maruš a Bradač, Anthony H. Gonzalez, et al. A direct empirical proof of the existence of dark matter. *The Astrophysical Journal*, 648(2):L109–L113, aug 2006. doi:10.1086/508162. URL https://doi.org/10.1086%2F508162.

[6] and N. Aghanim, Y. Akrami, M. Ashdown, et al. Planck 2018 results. *Astronomy & Astrophysics*, 641:A6, sep 2020. doi:10.1051/0004-6361/201833910. URL https://doi.org/10.1051%2F0004-6361%2F201833910.

[7] C. L. Bennett, D. Larson, J. L. Weiland, et al. NINE-YEAR WILKINSON MICROWAVE ANISOTROPY PROBE (WMAP) OBSERVATIONS: FINAL MAPS AND RESULTS. *The Astrophysical Journal Supplement Series*, 208(2):20, sep 2013. doi:10.1088/0067-0049/208/2/20. URL https://doi.org/10.1088%2F0067-0049%2F208%2F2%2F20.

[8] Ricardo A. Flores and Joel R. Primack. Observational and Theoretical Constraints on Singular Dark Matter Halos. *ApJ*, 427:L1, May 1994. doi:10.1086/187350.

[9] Ben Moore. Evidence against dissipation-less dark matter from observations of galaxy haloes. *Nature*, 370 (6491):629–631, Aug 1994. ISSN 1476-4687. doi: 10.1038/370629a0. URL https://doi.org/10.1038/370629a0.

[10] Karukes, E. V., Salucci, P., and Gentile, G. The dark matter distribution in the spiral ngc 3198 out to 0.22 rvir. *A&A*, 578:A13, 2015. doi:10.1051/0004-6361/201425339. URL https://doi.org/10.1051/0004-6361/201425339.

[11] Anatoly Klypin, Andrey V. Kravtsov, Octavio Valenzuela, and Francisco Prada. Where are the missing galactic satellites? *The Astrophysical Journal*, 522(1):82–92, sep 1999. doi:10.1086/307643. URL https://doi.org/10.1086%2F307643.

[12] Ben Moore, Sebastiano Ghigna, Fabio Governato, George Lake, Thomas Quinn, Joachim Stadel, and Paolo Tozzi. Dark Matter Substructure within Galactic Halos. *ApJ*, 524(1):L19–L22, October 1999. doi:10.1086/312287.

[13] Michael Boylan-Kolchin, James S. Bullock, and Manoj Kaplinghat. Too big to fail? The puzzling darkness of massive Milky Way subhaloes. *Monthly Notices of the Royal Astronomical Society*, 415(1):L40–L44, July 2011. doi:10.1111/j.1745-3933.2011.01074.x.

[14] Alfred Amruth, Tom Broadhurst, Jeremy Lim, et al. Einstein rings modulated by wavelike dark matter from anomalies in gravitationally lensed images. *Nature Astronomy*, 7(6):736–747, Jun 2023. ISSN 2397-3366. doi: 10.1038/s41550-023-01943-9. URL https://doi.org/10.1038/s41550-023-01943-9.

[15] Mariafelicia De Laurentis and Paolo Salucci. The accurate mass distribution of m87, the giant galaxy with imaged shadow of its supermassive black hole, as a portal to new physics. *The Astrophysical Journal*, 929 (1):17, apr 2022. doi:10.3847/1538-4357/ac54b9. URL https://dx.doi.org/10.3847/1538-4357/ac54b9.

[16] Raffaella Morganti. The many routes to agn feedback. *Frontiers in Astronomy and Space Sciences*, 4, 2017. ISSN 2296-987X. doi:10.3389/fspas.2017.00042. URL https://www.frontiersin.org/articles/10.3389/fspas.2017.00042.

[17] J. F. Navarro, V. R. Eke, and C. S. Frenk. The cores of dwarf galaxy haloes. *Monthly Notices of the Royal Astronomical Society*, 283(3):L72–L78, dec 1996. doi: 10.1093/mnras/283.3.l72. URL https://doi.org/10.

1093%2Fmnras%2F283.3.172.

[18] F. Governato, A. Zolotov, A. Pontzen, et al. Cuspy no more: how outflows affect the central dark matter and baryon distribution in Lambda cold dark matter galaxies. *Monthly Notices of the Royal Astronomical Society*, 422(2):1231–1240, 04 2012. ISSN 0035-8711. doi: 10.1111/j.1365-2966.2012.20696.x. URL https://doi.org/10.1111/j.1365-2966.2012.20696.x.

[19] Alyson M. Brooks, Michael Kuhlen, Adi Zolotov, and Dan Hooper. A baryonic solution to the missing satellites problem. *The Astrophysical Journal*, 765(1):22, feb 2013. doi:10.1088/0004-637X/765/1/22. URL https://dx.doi.org/10.1088/0004-637X/765/1/22.

[20] T. K. Chan, D. Kereš, J. Oñorbe, P. F. Hopkins, A. L. Muratov, C.-A. Faucher-Giguère, and E. Quataert. The impact of baryonic physics on the structure of dark matter haloes: the view from the FIRE cosmological simulations. *Monthly Notices of the Royal Astronomical Society*, 454(3):2981–3001, 10 2015. ISSN 0035-8711. doi:10.1093/mnras/stv2165. URL https://doi.org/10.1093/mnras/stv2165.

[21] Jose Oñorbe, Michael Boylan-Kolchin, James S. Bullock, et al. Forged in fire: cusps, cores and baryons in low-mass dwarf galaxies. *Monthly Notices of the Royal Astronomical Society*, 454(2):2092–2106, 10 2015. ISSN 0035-8711. doi:10.1093/mnras/stv2072. URL https://doi.org/10.1093/mnras/stv2072.

[22] J. I. Read, O. Agertz, and M. L. M. Collins. Dark matter cores all the way down. *Monthly Notices of the Royal Astronomical Society*, 459(3):2573–2590, 03 2016. ISSN 0035-8711. doi:10.1093/mnras/stw713. URL https://doi.org/10.1093/mnras/stw713.

[23] John R. Jardel and Karl Gebhardt. The dark matter density profile of the fornax dwarf. *The Astrophysical Journal*, 746(1):89, jan 2012. doi:10.1088/0004-637X/746/1/89. URL https://dx.doi.org/10.1088/0004-637X/746/1/89.

[24] Michael B. Green, J. H. Schwarz, and Edward Witten. *SUPERSTRING THEORY. VOL. 1: INTRODUCTION*. Cambridge Monographs on Mathematical Physics. 7 1988. ISBN 978-0-521-35752-4.

[25] Peter Svrcek and Edward Witten. Axions in string theory. *Journal of High Energy Physics*, 2006(06): 051–051, jun 2006. doi:10.1088/1126-6708/2006/06/051. URL https://doi.org/10.1088%2F1126-6708%2F2006%2F06%2F051.

[26] Asimina Arvanitaki, Savas Dimopoulos, Sergei Dubovsky, Nemanja Kaloper, and John March-Russell. String axiverse. *Physical Review D*, 81(12), jun 2010. doi:10.1103/physrevd.81.123530. URL https://doi.org/10.1103%2Fphysrevd.81.123530.

[27] Renée Hlozek, Daniel Grin, David J. E. Marsh, and Pedro G. Ferreira. A search for ultralight axions using precision cosmological data. *Phys. Rev. D*, 91:103512, May 2015. doi:10.1103/PhysRevD.91.103512. URL https://link.aps.org/doi/10.1103/PhysRevD.91.103512.

[28] Vid Iršič, Matteo Viel, Martin G. Haehnelt, James S. Bolton, and George D. Becker. First constraints on fuzzy dark matter from lyman-alpha forest data and hydrodynamical simulations. *Phys. Rev. Lett.*, 119:031302, Jul 2017. doi:10.1103/PhysRevLett.119.031302. URL https://link.aps.org/doi/10.1103/PhysRevLett.119.031302.

[29] Eric Armengaud, Nathalie Palanque-Delabrouille, Christophe Yèche, David J. E. Marsh, and Julien Baur. Constraining the mass of light bosonic dark matter using SDSS Lyman-alpha forest. *Monthly Notices of the Royal Astronomical Society*, 471(4):4606–4614, 07 2017. ISSN 0035-8711. doi:10.1093/mnras/stx1870. URL https://doi.org/10.1093/mnras/stx1870.

[30] Takeshi Kobayashi, Riccardo Murgia, Andrea De Simone, Vid Iršič, and Matteo Viel. Lyman-alpha constraints on ultralight scalar dark matter: Implications for the early and late universe. *Physical Review D*, 96 (12), dec 2017. doi:10.1103/physrevd.96.123514. URL https://doi.org/10.1103%2Fphysrevd.96.123514.

[31] Matteo Nori, Riccardo Murgia, Vid Iršič, Marco Baldi, and Matteo Viel. Lyman-alpha forest and non-linear structure characterization in Fuzzy Dark Matter cosmologies. *Monthly Notices of the Royal Astronomical Society*, 482(3):3227–3243, 10 2018. ISSN 0035-8711. doi:10.1093/mnras/sty2888. URL https://doi.org/10.1093/mnras/sty2888.

[32] Keir K. Rogers and Hiranya V. Peiris. Strong bound on canonical ultralight axion dark matter from the lyman-alpha forest. *Phys. Rev. Lett.*, 126:071302, Feb 2021. doi: 10.1103/PhysRevLett.126.071302. URL https://link.aps.org/doi/10.1103/PhysRevLett.126.071302.

[33] Kohei Hayashi, Elisa G. M. Ferreira, and Hei Yin Jowett Chan. Narrowing the mass range of fuzzy dark matter with ultrafaint dwarfs. *The Astrophysical Journal Letters*, 912(1):L3, apr 2021. doi: 10.3847/2041-8213/abf501. URL https://doi.org/10.3847%2F2041-8213%2Fabf501.

[34] Neal Dalal and Andrey Kravtsov. Excluding fuzzy dark matter with sizes and stellar kinematics of ultrafaint dwarf galaxies. *Phys. Rev. D*, 106:063517, Sep 2022. doi:10.1103/PhysRevD.106.063517. URL https://link.aps.org/doi/10.1103/PhysRevD.106.063517.

[35] Hsi-Yu Schive, Ming-Hsuan Liao, Tak-Pong Woo, Shing-Kwong Wong, Tzihong Chiueh, Tom Broadhurst, and W-Y. Pauchy Hwang. Understanding the core-halo relation of quantum wave dark matter from 3d simulations. *Phys. Rev. Lett.*, 113:261302, Dec 2014. doi: 10.1103/PhysRevLett.113.261302. URL https://link.aps.org/doi/10.1103/PhysRevLett.113.261302.

[36] Jiajun Zhang, Hantao Liu, and Ming-Chung Chu. Cosmological simulation for fuzzy dark matter model. *Frontiers in Astronomy and Space Sciences*, 5, 2019. ISSN 2296-987X. doi:10.3389/fspas.2018.00048. URL https://www.frontiersin.org/articles/10.3389/fspas.2018.00048.

[37] Andrei Khmelnitsky and Valery Rubakov. Pulsar timing signal from ultralight scalar dark matter. *Journal of Cosmology and Astroparticle Physics*, 2014(02):019, feb 2014. doi:10.1088/1475-7516/2014/02/019. URL https://dx.doi.org/10.1088/1475-7516/2014/02/019.

[38] N. K. Porayko and K. A. Postnov. Constraints on ultralight scalar dark matter from pulsar timing. *Physical Review D*, 90(6), sep 2014. doi: 10.1103/physrevd.90.062008. URL https://doi.org/10.1103%2Fphysrevd.90.062008.

[39] Nataliya K. Porayko, Xingjiang Zhu, Yuri Levin, et al. Parkes pulsar timing array constraints on ultralight scalar-field dark matter. *Physical Review D*, 98(10), nov 2018. doi:10.1103/physrevd.98.102002. URL https://doi.org/10.1103%2Fphysrevd.98.102002.

[40] Zi-Qing Xia, Tian-Peng Tang, Xiaoyuan Huang, Qiang

Yuan, and Yi-Zhong Fan. Constraining ultralight dark matter using the fermi-lat pulsar timing array. *Phys. Rev. D*, 107:L121302, Jun 2023. doi: 10.1103/PhysRevD.107.L121302. URL https://link.aps.org/doi/10.1103/PhysRevD.107.L121302.

[41] J. Antoniadis, P. Arumugam, S. Arumugam, et al. The second data release from the european pulsar timing array V. implications for massive black holes, dark matter and the early universe, 2023. URL https://doi.org/10.48550/arXiv.2306.16227.

[42] Jo Bovy and Scott Tremaine. On the local dark matter density. *The Astrophysical Journal*, 756(1):89, aug 2012. doi:10.1088/0004-637X/756/1/89. URL https://dx.doi.org/10.1088/0004-637X/756/1/89.

[43] J I Read. The local dark matter density. *Journal of Physics G: Nuclear and Particle Physics*, 41(6): 063101, may 2014. doi:10.1088/0954-3899/41/6/063101. URL https://dx.doi.org/10.1088/0954-3899/41/6/063101.

[44] S Sivertsson, H Silverwood, J I Read, G Bertone, and P Steger. The localdark matter density from SDSS-SEGUE G-dwarfs. *Monthly Notices of the Royal Astronomical Society*, 478(2):1677–1693, 04 2018. ISSN 0035-8711. doi:10.1093/mnras/sty977. URL https://doi.org/10.1093/mnras/sty977.

[45] Pablo F. de Salas. Dark matter local density determination based on recent observations. *Journal of Physics: Conference Series*, 1468(1):012020, feb 2020. doi:10.1088/1742-6596/1468/1/012020. URL https://dx.doi.org/10.1088/1742-6596/1468/1/012020.

[46] Fabrizio Nesti and Paolo Salucci. The dark matter halo of the milky way, ad 2013. *Journal of Cosmology and Astroparticle Physics*, 2013(07):016, jul 2013. doi:10.1088/1475-7516/2013/07/016. URL https://dx.doi.org/10.1088/1475-7516/2013/07/016.

[47] David E. Kaplan, Andrea Mitridate, and Tanner Trickle. Constraining fundamental constant variations from ultralight dark matter with pulsar timing arrays. *Physical Review D*, 106(3), aug 2022. doi: 10.1103/physrevd.106.035032. URL https://doi.org/10.1103%2Fphysrevd.106.035032.

[48] Xiao Xue, Zi-Qing Xia, Xingjiang Zhu, et al. High-precision search for dark photon dark matter with the parkes pulsar timing array. *Phys. Rev. Res.*, 4:L012022, Feb 2022. doi:10.1103/PhysRevResearch.4.L012022. URL https://link.aps.org/doi/10.1103/PhysRevResearch.4.L012022.

[49] J. Antoniadis, S. Babak, A.-S. Bak Nielsen, C. G. Bassa, A. Berthereau, et al. The second data release from the european pulsar timing array I. the dataset and timing analysis. *A&A*, jun 2023. doi: 10.1051/0004-6361/202346841. URL https://doi.org/10.1051%2F0004-6361%2F202346841.

[50] J. Antoniadis, P. Arumugam, S. Arumugam, et al. The second data release from the european pulsar timing array II. customised pulsar noise models for spatially correlated gravitational waves, 2023. URL https://doi.org/10.48550/arXiv.2306.16225.

[51] J. Antoniadis, P. Arumugam, S. Arumugam, et al. The second data release from the european pulsar timing array III. search for gravitational wave signals, 2023. URL https://doi.org/10.48550/arXiv.2306.16214.

[52] Rutger van Haasteren, Yuri Levin, Patrick McDonald, and Tingting Lu. On measuring the gravitational-wave background using Pulsar Timing Arrays. *Monthly Notices of the Royal Astronomical Society*, 395(2):1005–1014, May 2009. doi:10.1111/j.1365-2966.2009.14590.x.

[53] L. Lentati, P. Alexander, M. P. Hobson, F. Feroz, R. van Haasteren, K. J. Lee, and R. M. Shannon. TEMPONEST: a Bayesian approach to pulsar timing analysis. *Monthly Notices of the Royal Astronomical Society*, 437(3):3004–3023, January 2014. doi: 10.1093/mnras/stt2122.

[54] S. R. Taylor, L. Lentati, S. Babak, P. Brem, J. R. Gair, A. Sesana, and A. Vecchio. All correlations must die: Assessing the significance of a stochastic gravitational-wave background in pulsar timing arrays. *Phys. Rev. D*, 95(4):042002, February 2017. doi: 10.1103/PhysRevD.95.042002.

[55] Justin A. Ellis, Michele Vallisneri, Stephen R. Taylor, and Paul T. Baker. Enterprise: Enhanced numerical toolbox enabling a robust pulsar inference suite. Zenodo, September 2020. URL https://doi.org/10.5281/zenodo.4059815.

[56] Stephen R. Taylor, Paul T. Baker, Jeffrey S. Hazboun, Joseph Simon, and Sarah J. Vigeland. enterprise_extensions, 2021. URL https://github.com/nanograv/enterprise_extensions. v2.3.3.

[57] Justin Ellis and Rutger van Haasteren. jellis18/ptmcmcsampler: Official release, October 2017. URL https://doi.org/10.5281/zenodo.1037579.

[58] James M. Dickey. The weighted likelihood ratio, linear hypotheses on normal location parameters. *The Annals of Mathematical Statistics*, 42(1):204–223, 1971. ISSN 00034851. URL http://www.jstor.org/stable/2958475.

[59] Boris Goncharov, Eric Thrane, Ryan M. Shannon, et al. Consistency of the Parkes Pulsar Timing Array Signal with a Nanohertz Gravitational-wave Background. *ApJ*, 932(2):L22, June 2022. doi:10.3847/2041-8213/ac76bb.

[60] Joshua W. Foster, Nicholas L. Rodd, and Benjamin R. Safdi. Revealing the dark matter halo with axion direct detection. *Physical Review D*, 97(12), jun 2018. doi: 10.1103/physrevd.97.123006. URL https://doi.org/10.1103%2Fphysrevd.97.123006.

[61] Gary P. Centers, John W. Blanchard, Jan Conrad, et al. Stochastic fluctuations of bosonic dark matter. *Nature Communications*, 12(1), dec 2021. doi: 10.1038/s41467-021-27632-7. URL https://doi.org/10.1038%2Fs41467-021-27632-7.

[62] Jeffrey S. Hazboun, Joseph D. Romano, and Tristan L. Smith. Realistic sensitivity curves for pulsar timing arrays. *Phys. Rev. D*, 100(10):104028, November 2019. doi: 10.1103/PhysRevD.100.104028.

[63] R. Blandford, R. Narayan, and R. W. Romani. Arrival-time analysis for a millisecond pulsar. *Journal of Astrophysics and Astronomy*, 5:369–388, December 1984. doi:10.1007/BF02714466.

[64] Harikrishnan Ramani, Tanner Trickle, and Kathryn M. Zurek. Observability of dark matter substructure with pulsar timing correlations. *Journal of Cosmology and Astroparticle Physics*, 2020(12):033, dec 2020. doi:10.1088/1475-7516/2020/12/033. URL https://dx.doi.org/10.1088/1475-7516/2020/12/033.

[65] Caner Unal, Federico R. Urban, and Ely D. Kovetz. Probing ultralight scalar, vector and tensor dark matter with pulsar timing arrays, 2022. doi: https://doi.org/10.48550/arXiv.2209.02741

[66] Adeela Afzal, Gabriella Agazie, Akash Anumarlapudi, et al. The nanograv 15 yr data set: Search for signals from new physics. *The Astrophysical Journal Letters*, 951 (1):L11, jun 2023. doi:10.3847/2041-8213/acdc91. URL https://dx.doi.org/10.3847/2041-8213/acdc91.

[67] M T Miles, R M Shannon, M Bailes, et al. The MeerKAT pulsar timing array: first data release. *Monthly Notices of the Royal Astronomical Society*, 519(3):3976–3991, dec 2022. doi:10.1093/mnras/stac3644. URL https://doi.org/10.1093%2Fmnras%2Fstac3644.

[68] J. Antoniadis, P. Arumugam, S. Arumugam, et al. The second data release from the european pulsar timing array IV. search for continuous gravitational wave signals, 2023. URL https://doi.org/10.48550/arXiv.2306.16226.

[69] J. P. W. Verbiest, L. Lentati, G. Hobbs, R. van Haasteren, P. B. Demorest, G. H. Janssen, J. B. Wang, G. Desvignes, R. N. Caballero, M. J. Keith, D. J. Champion, et al. The International Pulsar Timing Array: First data release. *Monthly Notices of the Royal Astronomical Society*, 458(2):1267–1288, May 2016. doi:10.1093/mnras/stw347.